

VIP Very Important Paper

Discovery of Novel Allosteric Non-Bisphosphonate Inhibitors of Farnesyl Pyrophosphate Synthase by Integrated Lead Finding

Andreas L. Marzinzik,^{*[a]} René Amstutz,^[a, b] Guido Bold,^[a] Emmanuelle Bourgier,^[a] Simona Cotesta,^[a] J. Fraser Glickman,^[a, c] Marjo Götte,^[a] Christelle Henry,^[a] Sylvie Lehmann,^[a] J. Constanze D. Hartwig,^[a] Silvio Ofner,^[a] Xavier Pellé,^[a] Thomas P. Roddy,^[a, d] Jean-Michel Rondeau,^[a] Frédéric Stauffer,^[a] Steven J. Stout,^[a, e] Armin Widmer,^[a] Johann Zimmermann,^[a, f] Thomas Zoller,^[a] and Wolfgang Jahnke^{*[a]}

Farnesyl pyrophosphate synthase (FPPS) is an established target for the treatment of bone diseases, but also shows promise as an anticancer and anti-infective drug target. Currently available anti-FPPS drugs are active-site-directed bisphosphonate inhibitors, the peculiar pharmacological profile of which is inadequate for therapeutic indications beyond bone diseases. The recent discovery of an allosteric binding site has paved the way toward the development of novel non-bisphosphonate FPPS inhibitors with broader therapeutic potential, notably as immunomodulators in oncology. Herein we

report the discovery, by an integrated lead finding approach, of two new chemical classes of allosteric FPPS inhibitors that belong to the salicylic acid and quinoline chemotypes. We present their synthesis, biochemical and cellular activities, structure–activity relationships, and provide X-ray structures of several representative FPPS complexes. These novel allosteric FPPS inhibitors are devoid of any affinity for bone mineral and could serve as leads to evaluate their potential in none-bone diseases.

Introduction

Farnesyl pyrophosphate synthase (FPPS) is the main molecular target of nitrogen-containing bisphosphonates (N-BPs), one of the most transformative class of drugs of the past 25 years^[1] that had a huge impact on the treatment of bone diseases such as osteoporosis, Paget's disease of bone, and bone metastasis.^[2–4] FPPS is a key node of the mevalonate pathway and

provides the isoprenoid precursors geranyl- (GPP) and farnesyl- (FPP) pyrophosphate necessary for the synthesis of cholesterol, dolichol, and ubiquinone, and for post-translational prenylation of small GTPases such as Ras, Rac, and Rho. Bisphosphonate drugs such as zoledronic acid (**1**) (Scheme 1) strongly bind to bone and are then selectively taken up into bone-resorbing osteoclasts by fluid-phase endocytosis, subsequently inducing apoptosis and thereby inhibiting bone resorption.

[a] Dr. A. L. Marzinzik, Dr. R. Amstutz, Dr. G. Bold, E. Bourgier, Dr. S. Cotesta, Dr. J. F. Glickman, Dr. M. Götte, C. Henry, S. Lehmann, Dr. J. C. D. Hartwig, Dr. S. Ofner, X. Pellé, Dr. T. P. Roddy, Dr. J.-M. Rondeau, Dr. F. Stauffer, S. J. Stout, A. Widmer, Dr. J. Zimmermann, Dr. T. Zoller, Dr. W. Jahnke
Novartis Institutes for BioMedical Research
Basel, 4002 (Switzerland)
E-mail: wolfgang.jahnke@novartis.com
andreas.marzinzik@novartis.com

[b] Dr. R. Amstutz
Current address: Conim AG, Oberwiler Kirchweg 4c, 6300 Zug (Switzerland)

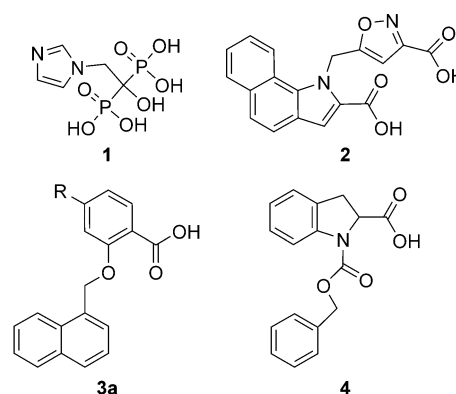
[c] Dr. J. F. Glickman
Current address: High Throughput and Spectroscopy Resource Center
Rockefeller University, New York, NY 10065 (USA)

[d] Dr. T. P. Roddy
Current address: Agios, Cambridge, MA 02139-4169 (USA)

[e] S. J. Stout
Current address: Merck Research Laboratories
126 E. Lincoln Avenue, Rahway, NJ, 07065 (USA)

[f] Dr. J. Zimmermann
Current address: Polyphor
Hegenheimertweg 125, 4123 Allschwil (Switzerland)

Supporting information for this article is available on the WWW under <http://dx.doi.org/10.1002/cmdc.201500338>.



Scheme 1. Structures of zoledronic acid **1** and selected allosteric FPPS inhibitors **2** and **4**, discovered by fragment-based screening.^[18] Compound **3** represents a series of new FPPS inhibitors that consist of a salicylic acid fragment substituted at C4.

Intriguingly, N-BPs have been found to exhibit a surprising variety of other pharmacological activities that include increased longevity in a mouse model of progeria,^[5] as well as antiviral^[6] and antiparasitic^[7] effects. In the clinic, antitumor effects have been observed in breast cancer^[8] and multiple myeloma^[9] patients. The exact mechanisms underlying the antitumor activity are not yet fully understood. They may include apoptosis of tumor cells due to increased demand for prenylation in rapidly proliferating cells, and activation of $\gamma\delta$ T cells by accumulating and presenting phospho-antigens such as isopentenyl pyrophosphate (IPP), one of the FPPS substrates.^[10,11] Both mechanisms involve FPPS inhibition, therefore pointing to FPPS as a potential novel drug target for direct antitumor therapy.

N-BPs have unusual pharmacokinetic (PK) properties characterized by rapid and strong binding to bone mineral, associated with low plasma drug concentration soon after administration, low permeability into non-endocytic cells, and low oral bioavailability.^[2] While this peculiar PK profile is a blessing for the treatment of bone diseases and contributes to the exceptional safety and potency of this class of drugs, it severely compromises the efficacy of N-BPs as antitumor drugs, for which high cell permeability and high plasma levels over an extended period of time are required.

Crystallographic analyses of human FPPS complexes with marketed N-BPs^[12,13] have revealed how these drugs mimic one of the FPPS substrates, dimethylallyl pyrophosphate (DMAPP), and explained why early attempts to move away from the bisphosphonate chemotype were largely unsuccessful.^[14] Currently marketed N-BPs are very small in size but are highly efficient inhibitors. The geminal bisphosphonate moiety of these drugs fills the site normally occupied by the pyrophosphate group of DMAPP, and plays a major role in recognition and binding through strong electrostatic interactions with a trinuclear Mg^{2+} center and three basic side chains: Arg112, Lys200, and Lys257. As all bisphosphonate oxygen atoms make important contributions to these interactions, modifying or replacing the bisphosphonate moiety by a less polar isostere long seemed virtually impossible, leaving the central carbon atom as the only available position for chemical elaboration of novel inhibitors. In particular, N-BPs with extended, lipophilic side chains exploiting the GPP/FPP pocket have been investigated, with the goal to expand the clinical utility of FPPS inhibitors.^[15–17]

With the same goal in mind, we initiated a drug discovery project aimed at novel FPPS inhibitors based on an *integrated lead finding* approach combining fragment-based screening (FBS), high-throughput screening (HTS), in silico screening, SAR-by-inventory, biophysical validation of hits, and hit-to-lead chemistry. The fragment-based screen rapidly identified the first allosteric non-bisphosphonate inhibitors of FPPS, and quickly led to the benzimidazole derivative **2** (Scheme 1), a novel, potent ($IC_{50} = 80$ nM) FPPS inhibitor devoid of avidity toward bone mineral.^[18] This part of our work has already been described in detail elsewhere.^[18] Building on these results, other research groups have recently reported further examples of non-bisphosphonate allosteric FPPS inhibitors.^[19–21]

Herein we describe two additional chemical lead series of allosteric FPPS inhibitors that were discovered during the course of our integrated lead finding efforts. These two series, salicylic acid and quinoline derivatives, are fivefold more potent in vitro than our first lead series represented by the benzimidazole derivative **2**, and are equally potent to the best bisphosphonates. They are again devoid of significant affinity toward bone mineral, and therefore represent interesting lead molecules for the treatment of non-bone-related diseases as anticancer or anti-infective agents.

In an accompanying report, we describe how such lead molecules can also be optimized for bone indications by fine-tuning their affinity toward bone mineral through covalent attachment of a suitable bone-affinity tag, while simultaneously retaining desirable properties such as oral bioavailability.^[22]

Results and Discussion

Discovery of the salicylic acid class of allosteric FPPS inhibitors

The fragment screen by NMR and fragment optimization work were performed so rapidly that compound **2** had already been discovered^[18] by the time the high-throughput screen was run. The HTS was based on a scintillation proximity assay (SPA) that monitored the incorporation of 3H -labeled IPP into [3H]farnesyl pyrophosphate ([3H]FPP) by capturing the latter onto a phosphatidylserine-coated scintillating microtiter plate ("flash-plate").^[23] In total, 850 000 compounds were screened at a concentration of 10 μM . The best non-bisphosphonate hits had IC_{50} values in the single-digit to double-digit micromolar range. Of particular interest was compound **3a** (Scheme 1, $R = H$), a salicylic acid derivative with an IC_{50} value of 54 μM in the SPA identified by a similarity search from a salicylic acid fragment identified by NMR. Although the activity of **3a** was close to the detection limit, we noticed that this hit shared some substructures (naphthyl and benzyloxy moiety, carboxylic acid functionality) with other NMR fragment hits or optimized allosteric inhibitors, such as **2** and **4** (Scheme 1). As this compound was also deemed chemically attractive, it was selected for follow-up validation and characterization studies.

FPPS was co-crystallized with **3a**, and the X-ray structure of the complex was determined. Crystallographic analysis confirmed that this hit was a genuine allosteric inhibitor of FPPS, binding to the same allosteric pocket as the previously identified NMR fragment hits, with the enzyme in the open state and the flexible C-terminal tail disordered (Figure 1A).^[12] This allosteric pocket is mainly lined by α -helices α_C , α_G , α_H , and α_I and also involves Tyr10 from helix α_A as well as Lys57 from the loop connecting helices α_B and α_C . The naphthyl group binds to the hydrophobic base of the pocket, making close contacts to Tyr10, Phe206, Phe239, Leu344, Thr63, and to the alkyl portion of the side chains of Lys347, Arg60, and Asn59 (Figure 1B). The side chain amide of Asn59 is in a parallel orientation with respect to the naphthyl group and contributes amide- π stacking interactions. The salicylic acid ring forms a face-to-edge aromatic-aromatic interaction with Phe239, while one carboxylic

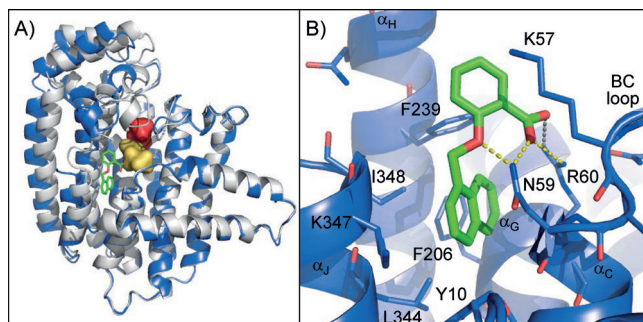
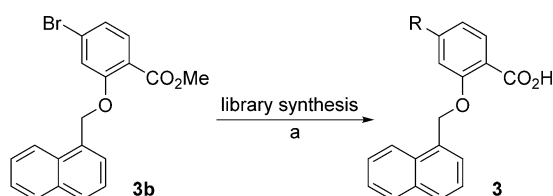


Figure 1. Crystal structure of the binary complex of FPPS with the allosteric inhibitor **3a**. A) Overall view of one FPPS subunit showing the location of the allosteric site (green stick) in relation to the DMAPP/ZOL (red) and IPP (yellow) binding sites. Note the different conformational states adopted by the enzyme in the binary complex with **3a** (open state, blue ribbon) and in the ternary complex with ZOL and IPP^[12] (closed state, gray ribbon). B) Close-up view of the complex with **3a** (green stick) with protein side chains within 4.0 Å distance shown in blue stick.

oxygen atom and the ether oxygen engage in short hydrogen bonding contacts with the side chain amide of Asn59. In addition, the carboxylic group makes strong electrostatic interactions with Arg60 (Figure 1B). The side chain amino group of Lys57 forms a cation- π interaction with the aromatic ring of the salicylic acid group.

To guide the optimization of **3a**, a virtual library of 17 000 salicylic acid analogues was created, and high-throughput docking simulations into FPPS were performed using the crystal structure of the complex with **3a** as a template. The virtual library allowed substitutions at the salicylic acid and naphthyl rings, and for α and β linkage of the naphthyl ring. Analysis of the results of the docking simulations indicated that the α -linked naphthyl ring fit the allosteric pocket best. Regarding the salicylic acid ring, the position *para* to the carboxylic acid seemed to offer the best opportunities for improvement. Therefore, we decided to prepare the key intermediate **3b** with a bromine at this position that could be used as a starting point for the parallel synthesis of derivatives by Suzuki coupling or Buchwald-Hartwig amination (Scheme 2). The resulting derivatives were tested in an LC-MS-based biochemical assay (see Supporting Information), and their IC_{50} values were determined (Table 1). In this assay, **3a** had an IC_{50} value of 6.8 μM . Gratifyingly, these efforts resulted in several improved FPPS inhibitors with IC_{50} values in the double-digit nanomolar range. Notably, 4-substituted phenyl groups were particularly



Scheme 2. Synthesis of the salicylic acid library. *Reagents and conditions:* a) 1. boronic acid, Pd(PPh₃)₂Cl₂, Na₂CO₃, DME/EtOH/H₂O, MW (110 °C), 10 min, 2. LiOH, MeOH/THF, MW (120 °C), 12 min.

Table 1. Inhibition of human FPPS by salicylic acid derivatives.

Compd	R	IC_{50} [μM] ^[a]
3a	H	6.8
3c		20
3d		0.85
3e		0.25
3f		0.058
3g		0.038
3h		0.049
3i		0.080
3j		1.23
3k		0.19
3l		0.27
3m		0.11
3n		0.017
3o		0.14

[a] Determined by LC-MS assay; all values are the average of at least three independent measurements.

efficient in enhancing binding affinity, with the 4-acetamidophenyl derivative **3n** showing a 400-fold improvement over the parent compound **3a**. The activity of the 6-methoxynaphthyl derivative **3g** was similar to that of **3n**. The *N*-methylindole derivative **3l** was selected for isothermal titration calorimetry (ITC) analysis. Enthalpically driven binding was observed ($-8.03 \text{ kcal mol}^{-1}$) with a favorable entropic contribution ($+3.10 \text{ kcal mol}^{-1} \text{ K}^{-1}$) and an estimated K_D value of 280 nM, well in line with the IC_{50} value in the LC-MS assay. However, these salicylic acid derivatives were, at best, only weakly active in a cellular plasma membrane translocation assay.^[24] With an IC_{50} value of 20 μM , compound **3i** was found to be among the most active compounds in this cellular assay. The poor cellular permeability of this compound series, resulting from the carboxylic acid functionality, probably precluded a higher cellular potency.

Discovery of the quinoline class of allosteric FPPS inhibitors

A third lead series emerged from our integrated lead finding efforts. Compound **5**, an HTS hit with an IC_{50} value of 7.1 μM in the LC-MS assay, also attracted our attention because of its fragment-like character ($M_r=287 \text{ Da}$), its relatively good ligand efficiency (LE: 0.32), and its structural features which suggested, in light of our previous results, that this compound might be an allosteric inhibitor as well. A crystal structure of **5** in complex with FPPS could be obtained, indeed revealing clear electron density for **5** bound to the allosteric site. Remarkably, the mode of binding of **5** was highly similar to that of **3a**, as demonstrated by a structural overlay (Figure 2A). The naphthyl groups of the two ligands superimpose with each other almost exactly. The indole moiety of **5** made an angle of 63.5° with respect to its naphthyl group, placing the carboxylic acid in the same location as its counterpart in compound **3a**. The two carboxylic groups showed a distinct orientation, but one of their oxygen atoms, the one closest to Arg60, virtually superimposed in the two complexes (Figure 2A). In spite of the short connection to the naphthyl group, the indole moiety of **5**, like the salicylic acid ring of **3a**, formed favorable face-to-edge aromatic-aromatic interactions with Phe239. Thus, compound **5** appeared as an attractive, more compact, rigid analogue of **3a**. Interestingly, **5** was not able to form the set of strong hydrogen bonding interactions with Asn59 that were a recurring feature of many FPPS complexes with allosteric inhibitors observed thus far, including compound **3a** in particular. The carboxylic acid group of **5** was rotated away from this residue. Furthermore, **5** did not have any counterpart for the ether oxygen atom of **3a**. The C3 atom rather than the indole nitrogen was in close contact (3.2 Å) with Asn59, as a consequence of the attachment of the naphthyl group at position 4, rather than 7, of the indole six-membered ring. Moreover, the indole nitrogen atom did not seem to form any direct polar contacts with FPPS. Hence, compound **5** also showed clear potential for affinity improvement, as its indole-carboxylate/naphthyl scaffold seemed suboptimal.

In a first step, we therefore looked for a better combination of ring systems using the corresponding non-decorated scaffold.

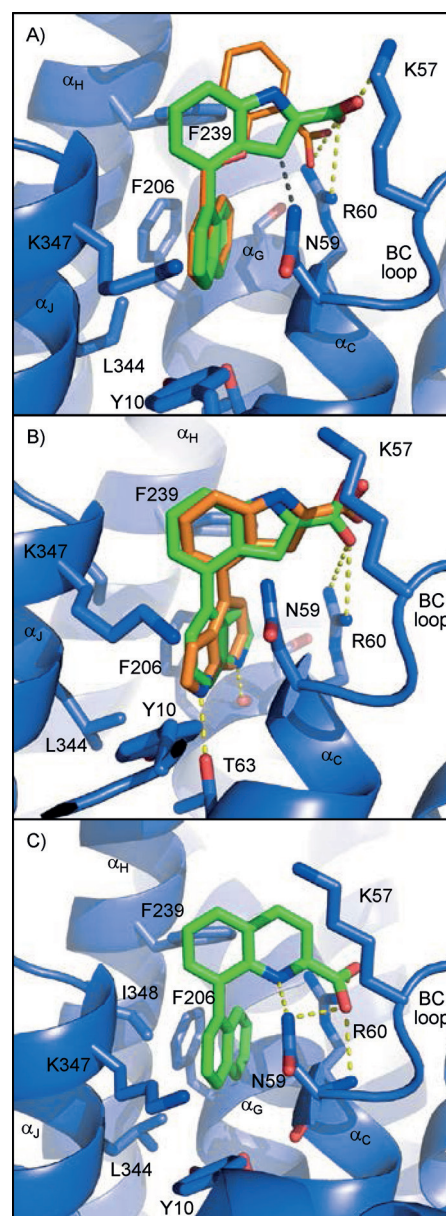
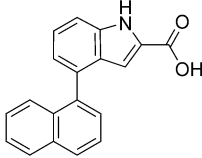
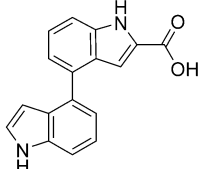
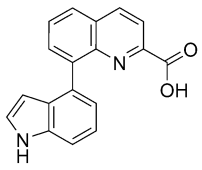
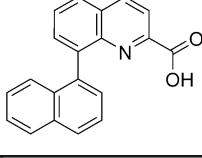


Figure 2. Crystal structures of FPPS in complex with A) compound **5** (green carbon atoms), also showing a structural overlay with compound **3a** (orange); B) compound **6**, observed in two alternate conformations (green and orange models); C) compound **8a** (green). Protein side chains within 4.0 Å distance of the allosteric inhibitor are shown in blue stick. See text for details.

Replacing the naphthyl group with an indole (compound **6**, Table 2) slightly weakened the activity to 13.9 μM . Instead, retaining the naphthyl group and replacing the indole carboxylate with a quinoline carboxylate with the naphthyl attached at position 8 of the quinoline system led to a clear improvement in potency (compound **8a**, $IC_{50}=1.2 \mu\text{M}$), whereas replacing the naphthyl group in **8a** with an indole to form compound **7** again decreased the activity to 20 μM (Table 2). The crystal structure of the FPPS complex with **6** confirmed that an indole moiety was not a snug fit into the base of the allosteric pocket, and therefore not a suitable replacement for the naphthyl group. The observed electron density indicated the pres-

Compd	IC ₅₀ [μM] ^[a]
	7.1
	13.9
	20.0
	1.2

[a] Determined by LC-MS assay; all values are the average of at least three independent measurements.

ence of two alternate binding modes, corresponding to opposite orientations of the buried indole group (Figure 2B). In one orientation, the indole nitrogen atom was within hydrogen bonding distance of Thr63 O_γ, while in the other orientation it appeared to interact with Ser205 O. In contrast, the crystal structure of the FPPS complex with the quinoline derivative **8a** confirmed that an 8-substituted quinoline 2-carboxylic acid group was a better match to the binding site than the original 4-substituted indole 2-carboxylic acid of **5** (Figure 2C). In particular, the hydrogen bonding interactions involving Asn59 were largely restored in this complex. The quinoline nitrogen was engaged in a short (2.6 Å) hydrogen bonding contact to Asn59 Nδ2, and one carboxylic acid oxygen atom appeared to form a bifurcated hydrogen bond with the main chain nitrogen (2.9 Å) as well as with the side chain amide (3.1 Å) of Asn59. The analysis of this X-ray structure also suggested that suitable substituents at positions 5 or 6 of the quinoline group may increase binding affinity.

Synthesis of biaryl and quinoline derivatives

The synthesis of compounds **5** and **6** is shown in Scheme 3, and the synthesis of **7** and **8a** is shown in Scheme 4. Esterification of 8-hydroxyquinoline-2-carboxylic acid under Mitsunobu conditions gave the benzyl ester **10**. The 8-hydroxy functionality was converted into the boron pinacolate **12**, which was cou-

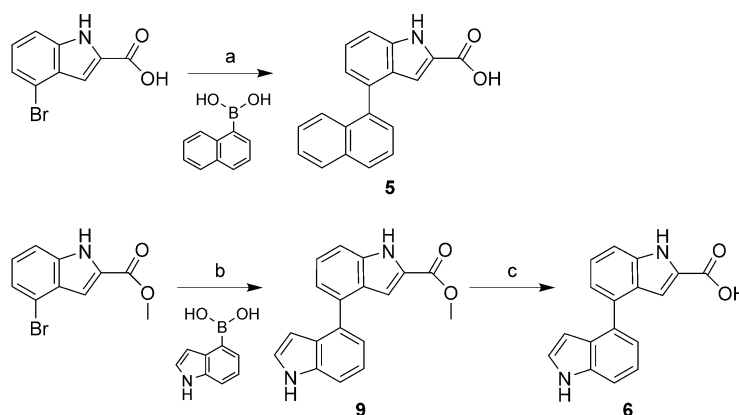
pled under palladium catalysis to the biaryl systems **14** and **13**. Transfer hydrogenation with ammonium formate and palladium on charcoal yielded the corresponding acids **7** and **8a**.

A variety of quinoline derivatives were then synthesized. Scheme 5 illustrates the synthesis of the 6-amino-8-(naphthalen-1-yl)quinoline-2-carboxylic acid derivatives **8c**, **8d**, and **8f**. Nitration of 8-bromoquinoline-2(1*H*)-one^[25] in a boiling mixture of fuming nitric and acetic acids occurs preferably at the 6-position.^[26] However, in our hands the reaction was dangerously exothermic under the described conditions. By exchanging the acetic acid for trifluoroacetic acid this nitration could be safely executed at or below room temperature. Suzuki coupling of the crude nitro derivative **15** with naphthyl boronate then gave **16**. Chlorination with POCl₃ in the presence of *N,N*-dimethylaniline and Et₄NCl^[27] yielded **17**. Palladium-catalyzed carbonylation of **17** was accompanied by reduction of the nitro group, yielding a mixture of products from which the 6-amino-2-ethoxycarbonyl derivative **18** was isolated in moderate yield. Additionally, **19** and **20** were isolated as side products. Saponification finally gave the corresponding acids **8c**, **8d**, and **8f**.

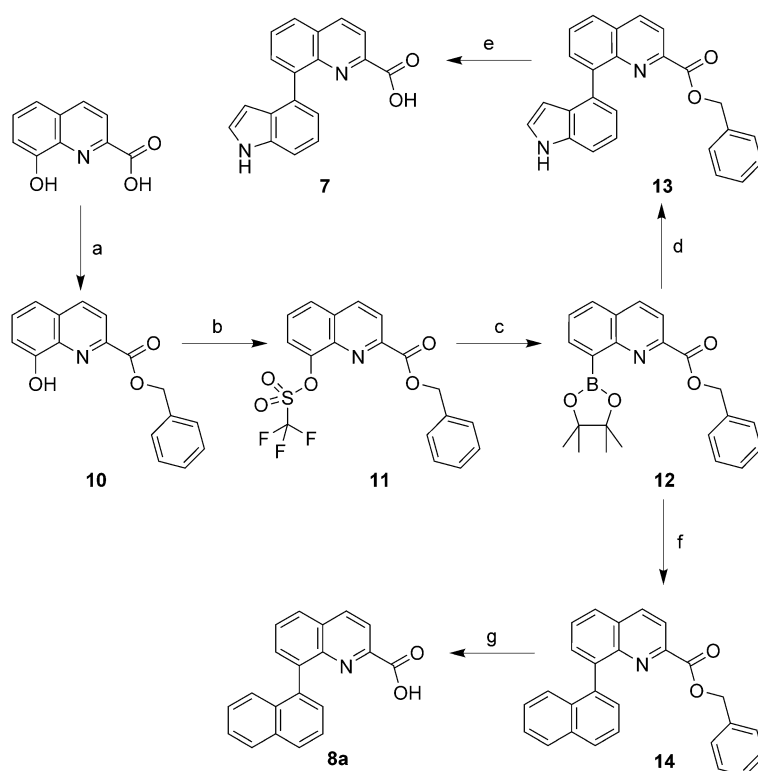
The 6-aryl-8-(naphthalen-1-yl)quinoline-2-carboxylic acid derivatives **8b** and **8e** were synthesized as depicted in Scheme 6: Sandmeyer-type conditions transformed **18** into the iodide **21**, which was cross-coupled with aryl-3-boronic acids to give **22** or **23**. Saponification or acidic hydrolysis and cleavage of the Boc protecting group finally lead to **8b** or **8e**, respectively.

SAR of quinoline derivatives

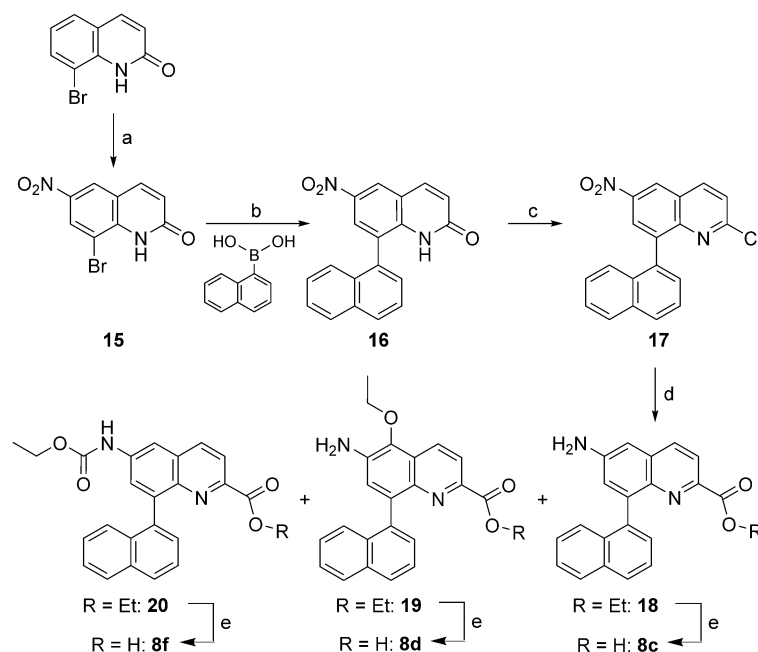
The inhibitory potencies of all quinoline derivatives were evaluated by LC-MS biochemical assay (Table 3). As with the salicylic acid series, low double-digit nanomolar activity against human FPPS was achieved with the most potent compounds, **8c-f**. By comparison, zoledronic acid showed an IC₅₀ value of 150 nM under the same experimental conditions (without pre-incubation). X-ray analysis of the FPPS complex with **8e** confirmed a conserved mode of binding with respect to the parent compound **8a**, with additional contacts involving the pyrrole sub-



Scheme 3. Synthesis of **5** and **6**. Reagents and conditions: a) Na₂CO₃, [(C₆H₅)₃P]₄Pd, EtOH, 3 h, reflux 80%; b) Na₂CO₃, [(C₆H₅)₃P]₄Pd, dioxane, 12 h, 90 °C, 44%; c) NaOH, MeOH, 2 h, 60 °C 48%.



Scheme 4. Synthesis of **7** and **8a**. *Reagents and conditions:* a) benzyl alcohol, $P(C_6H_5)_3$, diethyl azodicarboxylate, THF, $0^\circ C$ (88%); b) $(F_3CSO_2)_2O$, pyridine, CH_2Cl_2 /dioxane, $-78^\circ C \rightarrow RT$ (~quant.); c) bis(pinacolato)diboron, KOAc, molecular sieves (4 Å), [1,1'-bis(diphenylphosphino)ferrocene]palladium(II) chloride, DMF, $80^\circ C$; d) 4-bromoindole, Cs_2CO_3 , $[(C_6H_5)_3P]_4Pd$, DMF, $80^\circ C$ (50%, two steps); e) ammonium formiate, Pd/C, MeOH, $65^\circ C$ (83%); f) 1-bromonaphthalene, K_2CO_3 , $[(C_6H_5)_3P]_4Pd$, toluene, $90^\circ C$ (56%, two steps); g) ammonium formiate, Pd/C, MeOH, $65^\circ C$ (89%).



Scheme 5. Synthesis of **8c**, **8d**, and **8f**. *Reagents and conditions:* a) fuming HNO_3 , TFA, $0^\circ C \rightarrow RT$; b) K_2CO_3 , $[(C_6H_5)_3P]_2PdCl_2$, DMF/ H_2O , $80-92^\circ C$ (57%, two steps); c) $POCl_3$, Et_4NCl , *N,N*-dimethylaniline, CH_3CN , $\uparrow \downarrow$ (78%); d) CO, $[(C_6H_5)_3P]_2PdCl_2$, Et_3N , EtOH, $110^\circ C$; e) LiOH, H_2O /dioxane (31–63%).

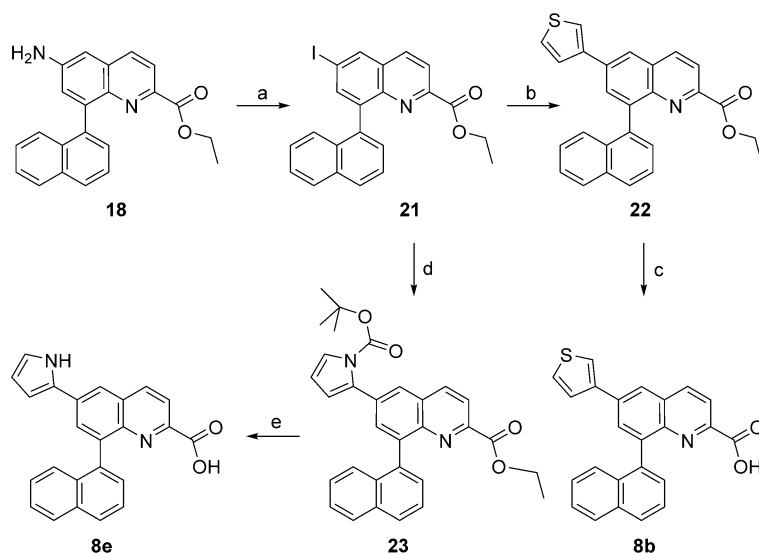
stituent. However, also with this series, cellular activities were found to be in the double-digit micromolar range, presumably due to poor permeability. Attempts to replace the carboxylic acid by a tetrazole met with limited success in the cellular assay.

Conclusions

FPPS is a highly validated drug target with an armamentarium of safe and highly efficient approved drugs. However, all the currently available anti-FPPS drugs belong to the same class, the so-called nitrogen-containing bisphosphonates (N-BPs). The unique pharmacokinetic properties of this class of drugs, dominated by its avidity to bone mineral, has largely restricted its use to bone related indications, including metastatic bone diseases. Nevertheless, evidence has been accumulating over the past decade that FPPS inhibitors have a much broader potential as cancer chemotherapeutic agents.^[28–32]

To fully realize this potential, however, novel non-bisphosphonate FPPS inhibitors are needed. This objective seemed elusive for a long time, as the first X-ray analyses had confirmed that N-BPs were substrate mimetics and had indicated that the design of non-bisphosphonate substrate analogues as a rational approach toward new FPPS inhibitors was doomed. The recent discovery of allosteric FPPS inhibitors, however, has revolutionized the field and opened new avenues toward the development of novel classes of anti-FPPS drugs.

This article complements the available chemical matter for allosteric inhibition of FPPS by two new lead series. These new classes were discovered by an integrated lead finding approach, which was essential for the rapid identification and characterization of promising, but



Scheme 6. Synthesis of **8b** and **8e**. Reagents and conditions: a) 1. NaNO₂, HCl, H₂O, -15 °C, 2. KI, 0 °C → RT (28%); b) thiophen-3-boronic acid; Na₂CO₃, [(C₆H₅)₃P]₂PdCl₂, DMF, 100 °C (81%); c) LiOH, H₂O/dioxane (83%); d) [1-(*tert*-butoxycarbonyl)-1*H*-pyrrol-2-yl]boronic acid, Na₂CO₃, [(C₆H₅)₃P]₂PdCl₂, DMF, 100 °C (69%); e) 2 M HCl in THF/H₂O (1:1), 50 °C (38%).

Table 3. Structures and FPPS inhibitory activities of analogues **8**.

Compd	R ¹	R ²	IC ₅₀ [μM] ^[a]
8a	H	H	1.2
8b		H	0.10
8c	NH ₂	H	0.069
8d	NH ₂	OEt	0.024
8e		H	0.077
8f		H	0.037

[a] Determined by LC-MS assay; all values are the average of at least three independent measurements.

weak hits from a high-throughput screen. In particular, the knowledge we had gained from our initial fragment-based work greatly helped us focus on a few compounds that exhibited the expected pharmacophore for putative new allosteric site binders.

One of the best inhibitors of our previous benzimidazole lead series, compound **2**, had an IC₅₀ value of 200 nM in the scintillation proximity assay.^[18] In our new LC-MS-based assay, which was used throughout the current study, compound **2** showed an IC₅₀ value of 350 nM. The two new classes reported herein

comprise compounds that are 10- to 20-fold more potent than the initial lead series. These compounds are exemplified by **3f** and **3n** for the salicylic acid series, and by **8d** and **8f** for the quinoline series.

Notably, the *in vitro* potencies of these allosteric inhibitors are in the same range or even higher than those of the most potent N-BPs, even if the latter are pre-incubated with FPPS before the start of the reaction, which increases their activities by a factor of 10–100.^[33] Moreover, both classes of FPPS inhibitors lack the bisphosphonate functionality and are thus radically distinct from the N-BPs. The bisphosphonate moiety is the “bone hook” that targets these drugs to bone, thus compromis-

ing their broader utility for non-skeletal indications. Allosteric inhibitors of FPPS, in contrast, are not substrate mimetics and therefore do not require a bisphosphonate group for binding affinity. With this major limitation of the N-BP class circumvented, and also in view of their relatively small size, there is still ample room for further chemical elaboration of these allosteric inhibitors, and, in particular, for improving their permeability and pharmacokinetic properties. So far, the cellular activity of our allosteric inhibitors in the membrane translocation assay was disappointing, with the best IC₅₀ values in the double-digit micromolar range. Nevertheless, this is a first step forward in comparison with N-BP drugs, such as zoledronic acid.

The allosteric binding site of FPPS is relatively basic owing to its vicinity to the IPP binding site, the nearby basic C-terminal tail of the enzyme with the sequence motif ³⁵⁰KRRK³⁵³, and the presence of several positively charged residues—Arg60, Lys57, and Lys347—within the pocket itself. Not too surprisingly, our best allosteric inhibitors feature at least one carboxylic acid functionality, which is absolutely critical for binding affinity. While carboxylic acid groups do not necessarily preclude cell permeability and are found in a wide variety of common drugs, including in particular NSAIDs (aspirin, ibuprofen) and cholesterol-lowering agents (Lipitor, Lescol, Crestor), further medicinal chemistry efforts are clearly required to develop one of these three series of allosteric FPPS inhibitors into a useful drug. A number of potential bioisosteres of carboxylic acid have been described,^[34] and prodrug approaches for carboxylic acids are also well documented.^[35] Pursuing all available options appears to be a very worthwhile endeavor. An allosteric FPPS drug should prove useful for a broad range of important indications with significant medical unmet needs. In oncology, the direct antitumor effects, synergistic effects with existing chemotherapies, as well as indirect immunostimulatory antitumor effects observed with zoledronic acid and other N-BPs

hold great promise for a next-generation allosteric FPPS drug with a superior pharmacokinetic profile. In addition, such a drug may prove useful as a novel cholesterol-lowering agent and whenever excessive lipid production causes disease, either by excessive prenylation of target proteins or overproduction of downstream products by the mevalonate pathway. As one example, the involvement of this pathway in human premature aging has raised the possibility of developing FPPS inhibitors for the treatment of devastating human progeria syndromes. Last but not least, the allosteric FPPS inhibitors reported herein may also serve as lead molecules for the development of new anti-parasitic agents, notably for the treatment of Chagas disease, malaria, and leishmaniasis, which affect several million people worldwide. For all of these indications, bisphosphonates have shown activity as tool compounds, again demonstrating the value of FPPS as a therapeutic target, but they are hardly suitable as drugs. While it is still unclear if the allosteric pocket of FPPS has any natural ligand or function, exploiting the Achilles' heel of this important therapeutic target will remain a fascinating scientific and medical endeavor for years to come.

Acknowledgements

The authors are grateful to Peggy Lefevre for performing the ITC analysis of compound **3l**, to Dr. Kazuhide Konishi for the synthesis of intermediate **3b**, to Christian Zwingelstein for the synthesis of compound **6**, and to Werner Beck, Ursula Dürler, Mario Madörin, and Christian Ragot for the synthesis of compounds **7** and **8a–f**. We thank Martin Geiser, Sebastien Rieffel, André Strauss, and René Hemmig for the cloning, expression, and purification of human FPPS. The coordinates of the crystal structures presented herein have been deposited with the RCSB Protein Data Bank (www.rcsb.org, PDB codes 5DIQ (FPPS + **3a**), 5DJP (FPPS + **5**), 5DJR (FPPS + **6**), 5DGN (FPPS + **8a**), 5DJV (FPPS + **8e**).

Keywords: allosteric inhibitors · antitumor agents · anti-infective drug discovery · FPPS · immunomodulation · immunotherapy

- [1] A. S. Kesselheim, J. Avorn, *Nat. Rev. Drug Discovery* **2013**, *12*, 425–443.
- [2] R. G. G. Russell, N. B. Watts, F. H. Ebetino, M. J. Rogers, *Osteoporosis Int.* **2008**, *19*, 733–759.
- [3] M. J. Rogers, J. C. Crockett, F. P. Coxon, J. Monkonen, *Bone* **2011**, *49*, 34–41.
- [4] F. P. Coxon, K. Thompson, M. J. Rogers, *Curr. Opin. Pharmacol.* **2006**, *6*, 307–312.
- [5] I. Varela, S. Pereira, A. P. Ugalde, C. L. Navarro, M. F. Suárez, P. Cau, J. Cañaneros, F. G. Osorio, N. Foray, J. Cobo, F. de Carlos, N. Lévy, J. M. P. Freije, C. López-Otín, *Nat. Med.* **2008**, *14*, 767–772.
- [6] X. Wang, E. R. Hinson, P. Cresswell, *Cell Host Microbe* **2007**, *2*, 96–105.
- [7] R. Docampo, S. N. Moreno, *Curr. Drug Targets Infect. Disord.* **2001**, *1*, 51–61.
- [8] M. Gnant, B. Mlineritsch, H. Stoeger, G. Luschin-Ebengreuth, D. Heck, C. Menzel, R. Jakesz, M. Seifert, M. Hubalek, G. Pristauz, T. Bauernhofer, H. Eidtmann, W. Eiermann, G. Steger, W. Kwasny, P. Dubsy, G. Hochreiner, E. P. Forsthuber, C. Fesl, R. Greil, et al., *N. Engl. J. Med.* **2009**, *360*, 679–691.
- [9] G. J. Morgan, *Lancet* **2010**, *376*, 1989–1999.

- [10] K. Thompson, M. J. Rogers, *J. Bone Miner. Res.* **2004**, *19*, 278–288.
- [11] R. E. Hewitt, A. Lissina, A. E. Green, E. S. Slay, D. A. Price, A. K. Sewell, *Clin. Exp. Immunol.* **2005**, *139*, 101–111.
- [12] J.-M. Rondeau, F. Bitsch, E. Bourcier, M. Geiser, R. Hemmig, M. Kroemer, S. Lehmann, P. Ramage, S. Rieffel, A. Strauss, J. R. Green, W. Jahnke, *ChemMedChem* **2006**, *1*, 267–273.
- [13] K. L. Kavanagh, K. Guo, J. E. Dunford, X. Wu, S. Knapp, F. H. Ebetino, M. J. Rogers, R. G. Russell, U. Oppermann, *Proc. Natl. Acad. Sci. USA* **2006**, *103*, 7829–7834.
- [14] M. S. Marma, Z. Xia, C. Stewart, F. Coxon, J. E. Dunford, R. Baron, B. A. Kashemirov, F. H. Ebetino, J. T. Triffitt, R. G. G. Russell, C. E. McKenna, *J. Med. Chem.* **2007**, *50*, 5967–5975.
- [15] Y. Zhang, R. Cao, F. Yin, M. P. Hudock, R.-T. Guo, K. Krysiak, S. Mukherjee, Y.-G. Gao, H. Robinson, Y. Song, J. H. No, K. Bergan, A. Leon, L. Cass, A. Goddard, T.-K. Chang, F.-Y. Lin, E. Van Beek, S. Papapoulos, A. H.-J. Wang, T. Kubo, M. Ochi, D. Mukkamala, E. Oldfield, *J. Am. Chem. Soc.* **2009**, *131*, 5153–5162.
- [16] Y. Zhang, R. Cao, F. Yin, F.-Y. Lin, H. Wang, K. Krysiak, J.-H. No, D. Mukkamala, K. Houlihan, J. Li, C. T. Morita, E. Oldfield, *Angew. Chem. Int. Ed.* **2010**, *49*, 1136–1138; *Angew. Chem.* **2010**, *122*, 1154–1156.
- [17] Y.-S. Lin, J. Park, J. W. De Schutter, X. F. Huang, A. M. Berghuis, M. Sebag, Y. S. Tsantrizos, *J. Med. Chem.* **2012**, *55*, 3201–3215.
- [18] W. Jahnke, J.-M. Rondeau, S. Costesta, A. Marzinik, X. Pellé, M. Geiser, A. Strauss, M. Götte, F. Bitsch, R. Hemmig, C. Henry, S. Lehmann, J. F. Glickman, T. P. Roddy, S. J. Stout, J. R. Green, *Nat. Chem. Biol.* **2010**, *6*, 660–666.
- [19] a) S. Lindert, W. Zhu, Y.-L. Liu, R. Pang, E. Oldfield, J. A. McCammon, *Chem. Biol. Drug Des.* **2013**, *81*, 742–748; b) Y.-L. Liu, R. Cao, Y. Wang, E. Oldfield, *ACS Med. Chem. Lett.* **2015**, *6*, 349–354.
- [20] a) J. W. Schmidberger, R. Schnell, G. Schneider, *Acta Crystallogr. Sect. D* **2015**, *71*, 721; b) J. Liu, W. Liu, H. Ge, J. Gao, Q. He, L. Su, J. Xu, L.-q. Gu, Z.-s. Huang, D. Li, *Biochim. Biophys. Acta* **2014**, *1840*, 1051–1062.
- [21] J. W. De Schutter, J. Park, C. Y. Leung, P. Gormley, Y.-S. Lin, Z. Hu, A. M. Berghuis, J. Poirier, Y. S. Tsantrizos, *J. Med. Chem.* **2014**, *57*, 5764–5776.
- [22] W. Jahnke, G. Bold, A. Marzinik, S. Ofner, X. Pellé, S. Costesta, E. Bourcier, S. Lehmann, C. Henry, R. Hemmig, F. Stauffer, J. C. D. Hartweg, J. R. Green, J.-M. Rondeau, *Angew. Chem. Int. Ed.* **2015**, DOI: 10.1002/anie.201507064; *Angew. Chem.* **2015**, DOI: 10.1002/ange.201507064.
- [23] J. F. Glickman, A. Schmid, *Assay Drug Dev. Technol.* **2007**, *5*, 205–214.
- [24] M. Simonen, Y. Ibig-Rehm, G. Hofmann, J. Zimmermann, G. Albrecht, M. Magnier, V. Heidinger, D. Gabriel, *J. Biomol. Screening* **2008**, *13*, 456–467.
- [25] F. Cottet, M. Marull, O. Lefebvre, M. Schlosser, *Eur. J. Org. Chem.* **2003**, 1559–1568.
- [26] G. Leclerc, G. Marciniak, N. Decker, J. Schwartz, *J. Med. Chem.* **1986**, *29*, 2433–2438.
- [27] H. Harada, O. Asano, T. Kawata, T. Inoue, T. Horioe, N. Yasuda, K. Nagata, M. Murakami, J. Nagaoka, S. Kobayashi, I. Tanaka, S. Abe, *Bioorg. Med. Chem.* **2001**, *9*, 2709–2726.
- [28] J. R. Berenson, *Curr. Opin. Support Palliat. Care* **2011**, *5*, 233–240.
- [29] G. Morgan, A. Lipton, *Semin. Oncol.* **2010**, *37*, S30–40.
- [30] H. K. Koul, S. Koul, R. B. Meacham, *Prostate Cancer Prostatic Dis.* **2012**, *15*, 111–119.
- [31] D. Santini, V. Virzi, M. E. Fratto, F. Bertoldo, R. Sabbatini, R. Berardi, N. Calipari, D. Ottaviani, T. Ibrahim, *Curr. Cancer Drug Targets* **2010**, *10*, 46–54.
- [32] M. Gnant, P. Clézardin, *Cancer Treat. Rev.* **2012**, *38*, 407–415.
- [33] J. E. Dunford, A. A. Kwaasi, M. J. Rogers, B. L. Barnett, F. H. Ebetino, R. G. G. Russell, U. Oppermann, K. L. Kavanagh, *J. Med. Chem.* **2008**, *51*, 2187–2195.
- [34] C. Ballatore, D. M. Huryn, A. B. Smith III, *ChemMedChem* **2013**, *8*, 385–395.
- [35] H. Maag in *Prodrugs: Challenges and Rewards* (Eds.: V. J. Stella, R. T. Borchardt, M. J. Hageman, R. Oliyai, H. Maag, J. Tilley), Springer, New York, **2007**, pp. 3–30.

Received: July 30, 2015

Published online on September 18, 2015